J|A|C|S
ARTICLES
Published on Web 07/13/2006

Revealing Two-State Protein−Protein Interactions of Calmodulin by Single-Molecule Spectroscopy

Ruchuan Liu, Dehong Hu, Xin Tan, and H. Peter Lu*

Contribution from the Fundamental Science Directorate, Chemical Science Division, Pacific Northwest National Laboratory, P.O. Box 999, MSIN K8-88, Richland, Washington 99352

Received October 20, 2005; E-mail: peter.lu@pnl.gov

Abstract: We report a single-molecule fluorescence resonance energy transfer (FRET) and polarization study of conformational dynamics of calmodulin (CaM) interacting with a target peptide, C28W of a 28 amino acid oligomer. The C28W peptide represents the essential binding sequence domain of the Ca-ATPase protein interacting with CaM, which is important in cellular signaling for the regulation of energy in metabolism. However, the mechanism of the CaM/C28W recognition complex formation is still unclear. The amino-terminal (N-terminal) domain of the CaM was labeled with a fluorescein-based arsenical hairpin binder (FlAsH) that enables our unambiguous probing of the CaM N-terminal target-binding domain motions on a millisecond time scale without convolution of the probe-dye random motions. By analyzing the distribution of FRET efficiency between FlAsH labeled CaM and Texas Red labeled C28W and the polarization fluctuation dynamics and distributions of the CaM N-terminal domain, we reveal binding−unbinding motions of the N-terminal domain of the CaM in CaM/C28W complexes, which is strong evidence of a two-state binding interaction of CaM-mediated cell signaling.

Introduction

Single-molecule spectroscopy, probing one molecule at a time, offers the unique advantage of resolving the dynamics and inhomogeneity of conformational motions of proteins and protein complexes that are particularly crucial for understanding the networks of molecular interactions in specific cellular functions, such as cell signaling. In recent years, single-molecule characterizations have been extensively applied to diverse biological systems [1−4] and have brought out new information on intermediate conformational states, the distribution of multiple conformations, and the variety of interaction pathways.[5]

Calmodulin (CaM) is an intracellular calcium-sensing protein that is involved in a variety of cell-signaling pathways, including muscle contraction and energy metabolism.[6,7] With 148 residues, CaM has two globular domains, each of which can bind to two Ca^{2+} ions in response to an increase in the Ca^{2+} level and which are connected by an extended α-helical element often referred to as the central helix.[8−10] Both domains and the central helix undergo conformational changes upon Ca^{2+} and protein binding in the role of modulation of enzymatic function.[11] On time scales spanning many orders of magnitude, from nanoseconds to seconds, static studies in X-ray crystallography,[8,12−14] solution nuclear magnetic resonance,[15−18] and fluorescence [19−23] have all provided valuable information on the structure and conformational dynamics of CaM.[19,21,24−31] The wide range of time

(1) Moerner, W. E.; Orrit, M. *Science* **1999**, *283* (5408), 1670−1676.
(2) Nie, S.; Zare, R. N. *Annual Review of Biophysics and Biomolecular Structure* **1997**, *26*, 567−596.
(3) Weiss, S. Fluorescence Spectroscopy of Single Biomolecules. *Science* **1999**, *283* (5408), 1676−1683.
(4) For reviews, see: *Acc. Chem. Res*. (special issue on single molecule spectroscopy) **2005**, *38* (7).
(5) For a review, see: *Protein−Ligand Interactions*;Nienhaus, G. U., Ed.; Humana Press: New Jersey, 2005.
(6) Chin, D.; Means, A. R. *Trends in Cell Biology* **2000**, *10* (8), 322−328.
(7) James, P.; Vorherr, T.; Carafoli, E. *Trends Biochem. Sci.* **1995**, *20* (1), 38−42.
(8) Babu, Y. S.; Sack, J. S.; Greenhough, T. J.; Bugg, C. E.; Means, A. R.; Cook, W. J. *Nature* **1985**, *315*, 37−40.
(9) Chattopadhyaya, R.; Meadorl, W. E.; Means, A. R.; Quiocho, F. A. *J. Mol. Biol.* **1992**, *228* (4), 1177−1192.
(10) Kuboniwa, H.; Tjandra, N.; Grzesiek, S.; Ren, H.; Klee, C. B.; Bax, A. *Nature Structural Biology* **1995**, *2* (9), 768−776.
(11) Vetter, S. W.; Leclerc, E. *Eur. J. Biochem.* **2003**, *270*, 404−414.
(12) Drum, C. L.; Yan, S.-Z.; Bard, J.; Shen, Y.-Q.; Lu, D.; Soelaiman, S.; Grabarek, Z.; Bohm, A.; Tang, W.-J. *Nature* **2002**, *415*, 396−402.
(13) Meador, W. E.; Means, A. R.; Quiocho, F. A. *Science* **1992**, *257*, 1251−1255.
(14) Schumacher, M. A.; Rivard, A. F.; Bächinger, H. P.; Adelman, J. P. *Nature* **2001**, *410*, 1120−1124.
(15) Elshorst, B.; Hennig, M.; Försterling, H.; Diener, A.; Maurer, M.; Schulte, P.; Schwalbe, H.; Griesinger, C.; Krebs, J.; Schmid, H.; Vorherr, T.; Carafoli, E. *Biochemistry* **1999**, *38*, 12320−12332.
(16) Ikura, M.; Clore, G. M.; Gronenborn, A. M.; Zhu, G.; Klee, C. B.; Bax, A. *Science* **1992**, *256* (5057), 632−638.
(17) Osawa, M.; Tokumitsu, H.; Swindells, M. B.; Kurihara, H.; Orita, M.; Shibanuma, T.; Furuya, T.; Ikura, M. *Nature Structural Biology* **1999**, *6* (9), 819−824.
(18) Zhang, M.; Tanaka, T.; Ikura, M. *Nature Structural Biology* **1995**, *2* (9), 758−767.
(19) Chen, B.; Mayer, M. U.; Markillie, L. M.; Stenoien, D. L.; Squier, T. C. *Biochemistry* **2005**, *44*, 905−914.
(20) Chapman, E. R.; Alexander, K.; Vorherr, T.; Carafoli, E.; Storm, D. R. *Biochemistry* **1992**, *31*, 12819−12825.
(21) Small, E. W.; Anderson, S. R. *Biochemistry* **1988**, *27*, 7 (1), 418−428.
(22) Sun, H.; Squier, T. C. *J. Biol. Chem.* **2000**, *275* (3), 1731−1738.
(23) Yao, Y.; Squier, T. C. *Biochemistry* **1996**, *35*, 6815−6827.
(24) Chang, S.-L.; Szabo, A.; Tjandra, N. *J. Am. Chem. Soc.* **2003**, *125*, (37), 11379−11384.
(25) Baber, J. L.; Szabo, A.; Tjandra, N. *J. Am. Chem. Soc.* **2001**, *123*, 3953−3959.
(26) Evenäs, J.; Forsén, S.; Malmendal, A.; Akke, M. *J. Mol. Biol.* **1999**, *289*, 603−617.
(27) Johnson, J. D.; Snyder, C.; Walsh, M.; Flynn, M. *J. Biol. Chem.* **1996**, *271* (2), 761−767.
(28) Kasturi, R.; Vasulka, C.; Johnson, J. D. *J. Biol. Chem.* **1993**, *268* (11), 7958−7964.
(29) Malmendal, A.; Evenäs, J.; Forsén, S.; Akke, M. *J. Mol. Biol.* **1999**, *293*, 883−899.

10.1021/ja057005m CCC: $33.50

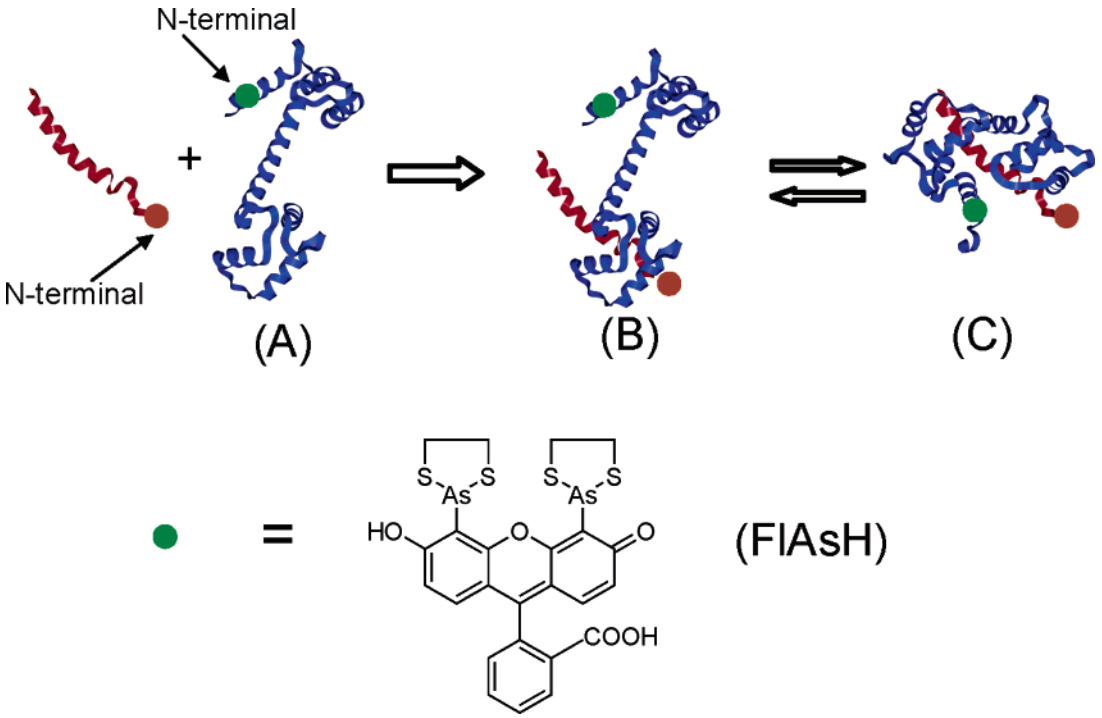

Figure 1. A cartoon model of the CaM and C28W interaction process: (A) CaM without C28W interaction; (B) the C-terminal domain of CaM binds to the N-terminal domain of C28W; (C) CaM tightly binds to C28W through both domains. The structures are derived from protein structure files (PDB: 1CLL, 1CFF, 2BBM) to illustrate the two-state interaction model.

scales and the conformational flexibility of CaM make single-molecule spectroscopy well suited for understanding CaM conformational changes and the dynamic rates of interconversion among its states. Recently, single-molecule techniques, such as fluorescence resonance energy transfer (FRET),[32] fluorescence anisotropy,[32,33] and polarization,[34,35] have been applied to characterize the conformational dynamics of CaM at millisecond[34,36] and sub-millisecond time scales,[32] and rotational lifetimes on a nanosecond time scale.[32,33] However, in most single-molecule studies of CaM, the conformational dynamics were convoluted with the labeled dye random motion relative to the CaM host, which often complicated the specificity of the probed conformational dynamics of CaM proteins, especially in protein interaction complexes.

FlAsH, a fluorescein-based arsenical hairpin binder derivative, can be selectively and rigidly attached to a tetra-cysteine binding motif, which can in turn be genetically fused or inserted within the protein.[37,38] This probe has recently been used to label CaM[19,39] and revealed CaM N-terminal domain motions without convoluting the probe-dye motion.[33] FlAsH is expected to be more extensively used in revealing structural and dynamic conformational changes and the inhomogeneity of proteins and protein complexes, including CaM and CaM/peptide complexes.

C28W is an oligomer of 28 amino acid residues, and it is the effective CaM-binding sequence of the plasma membrane Ca-ATPase.[40,41] A two-state model has been hypothesized for the CaM/C28W complex formation involving an intermediate state of either only the C-terminal domain bound to the peptide or both globular domains loosely bound to the peptide (as illustrated by the cartoons in Figure 1). Upon association of C28W with the binding cleft in the C-terminal domain of CaM (illustrated in Figure 1B), the N-terminal domain may bind around the target peptide. Figure 1C illustrates a possible example of the flexible conformational fluctuation of the N-domain binding to peptide targets. Although NMR measurements have provided some evidence to support the existence of the intermediate states, this hypothesized model is still being hotly debated[42] due to the lack of direct experimental evidence indicating the existence of and the fluctuations among the loosely bound and bound states (the two-state fluctuation of B ↔ C illustrated in Figure 1B and 1C).

In this paper, we report on (a) a single-molecule FRET study of interactions between FlAsH labeled CaM and Texas Red labeled C28W in solution and (b) a single-molecule fluorescence polarization study of nonlabeled C28W peptide interacting with FlAsH labeled CaM tethered to a biologically compatible surface. These two experiments were both conducted under three assay conditions: Ca^{2+} free CaM (apo-CaM), Ca^{2+}-activated CaM (Ca^{2+}-CaM), and complexes (CaM/C28W) of Ca^{2+}-activated CaM and C28W peptides. The distribution of FRET

(30) Peersen, O. B.; Madsen, T. S.; Falke, J. J. *Protein Science* **1997**, *6* (4), 794−807.
(31) Yao, Y.; Schöneich, C.; Squier, T. C. *Biochemistry* **1994**, *33*, 7797−7810.
(32) Slaughter, B. D.; Allen, M. W.; Unruh, J. R.; Urbauer, R. J. B.; Johnson, C. K. *J. Phys. Chem. B* **2004**, *108*, 10388−10397.
(33) Tan, X.; Hu, D.; Squier, T. C.; Lu, H. P. *Appl. Phys. Lett.* **2004**, *85* (12), 2420−2422.
(34) Tang, J.; Mei, E.; Green, C.; Kaplan, J.; DeGrado, W. F.; Smith, A. B., III; Hochstrasser, R. M. *J. Phys. Chem. B* **2004**, *108*, 15910−15918.
(35) Osborn, K. D.; Bartlett, R. K.; Mandal, A.; Zaidi, A.; Urbauer, R. J. B.; Urbauer, J. L.; Galeva, N.; Williams, T. D.; Johnson, C. K. *Biochemistry* **2004**, *43*, 12937−12944.
(36) Brasselet, S.; Peterman, E. J. G.; Miyawaki, A.; Moerner, W. E. *J. Phys. Chem. B* **2000**, *104*, 3676−3682.
(37) Adams, S. R.; Campbell, R. E.; Gross, L. A.; Martin, B. R.; Walkup, G. K.; Yao, Y.; Llopis, J.; Tsien, R. Y. *J. Am. Chem. Soc.* **2002**, *124* (21), 6063−6076.
(38) Griffin, B. A.; Adams, S. R.; Tsien, R. Y. *Science* **1998**, *281*, 269−272.
(39) Chen, B.; Mayer, M. U.; Squie, T. C. *Biochemistry* **2005**, *44* (12), 4737−4747.
(40) Vorherr, T.; James, P.; Krebs, J.; Enyedi, A.; McCormick, D. J.; Penniston, J. T.; Carafoli, E. *Biochemistry* **1990**, *29*, 355−365.
(41) Yao, Y.; Gao, J.; Squier, T. C. *Biochemistry* **1996**, *35*, 12015−12028.
(42) Kranz, J. K.; Flynn, P. F.; Fuentes, E. J.; Wand, A. J. *Biochemistry* **2002**, *41*, 2599−2608.

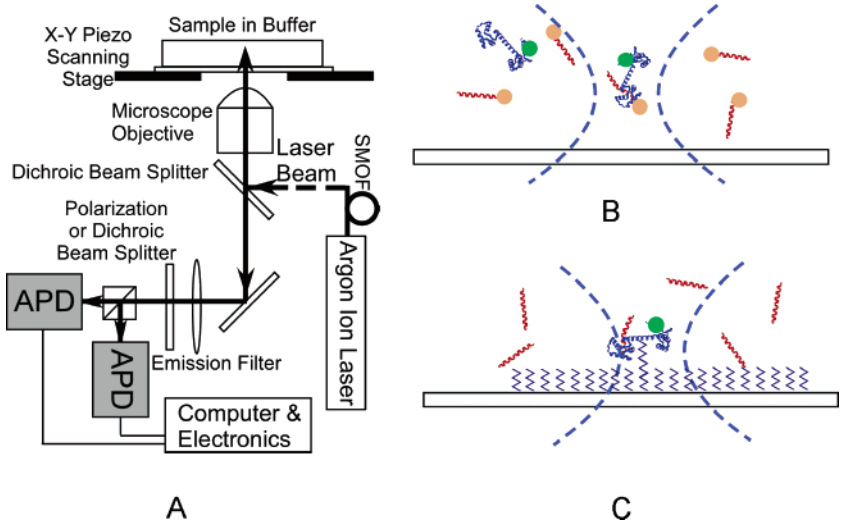

Figure 2. (A) Single-molecule fluorescence experimental scheme. Single-molecule measurements were performed on an inverted confocal fluorescence microscope (Zeiss Axiovert 200) with excitation light from a continuous-wave argon ion laser. Fluorescence photons were directed onto avalanche photodiodes (APDs) to acquire emission images and time trajectories. (B) Single-molecule FRET experiments. FlAsH labeled CaM and Texas Red labeled C28W both dissolved in buffer solution. (C) Single-molecule polarization experiments. Individual FlAsH labeled CaM proteins tethered to a biologically compatible glass surface were located by confocal laser raster-scanning.

efficiency was analyzed to reveal the distance of fluctuations between the N-terminal domains of CaM with C28W. The autocorrelation function of the fluorescence polarization was calculated to characterize the fluctuations of the N-terminal domain motion dynamics for the single FlAsH labeled CaM. The results were statistically analyzed and compared among the CaM and CaM/peptide conformational dynamics.

Materials and Methods

1. Chemicals and Sample Preparation. FlAsH labeled CaM protein was used in our experiments. A tetra-cysteine motif was genetically inserted at the 6, 7, 10, and 11 residue positions within an α-helix A near the amino terminus (N-terminal) of the CaM protein (Figure 1) and then reacted with FlAsH, a fluorescein derivative with two As(III) substituents.[19,33,37,38] The FlAsH fluoresced only after the arsenics bound to cysteine thiols,[37,38] ensuring that we were not detecting the free FlAsH molecules but those labeled on the CaM proteins. Ensemble-averaged CaM assays have definitively proven that the rigid FlAsH labeling at the N-terminal of the CaM has no impact and there is no perturbation of the CaM peptide recognition and binding capability.[19,39] The Texas Red labeled C28W peptide, Texas Red-L-R-R-G-Q-I-L-W-F-R-G-L-N-R-I-Q-T-Q-I-R-V-V-N-A-F-S-S-S (Global Peptide), was used together with the FlAsH labeled CaM in the single-molecule FRET experiments in solution.

In the single-molecule FRET experiments, a home-built assay cell (~80 μL) was used to hold the sample solution and the mixture of FlAsH labeled CaM (~400 pM) and Texas Red labeled C28W (~10 nM) in HEPES buffer (20 mM HEPES, 100 mM KCl, 5 mM $MgCl_2$, pH 7.5). Control measurements were conducted on solutions of FlAsH labeled CaM, Texas Red labeled C28W, and HEPES buffer, respectively.

For single-molecule fluorescence polarization measurements, the FlAsH labeled CaM and the nonlabeled C28W were used. The CaM was tethered through a bifunctional linker molecule[33,43] to a hydrocarbon-modified glass coverslip surface. The glass coverslips were first treated overnight with a 10% (v/v) mixture of 3-mercaptopropyl-trimethoxysilane and isobutyltrimethoxysilane ($1:10^4$ ratio) in DMSO. After washing with methanol and water, coverslips were incubated in 10 nM SIAXX (Molecular Probes, S-1668) in PBS buffer (pH 7.2) for 1 h. The thiol-reactive group of SIAXX attaches to the glass surface. After additional washing, the coverslips were incubated with 1 nM protein in 0.2 M bicarbonate buffer (pH 8.2) for 1 h followed by rinsing with water and a bicarbonate buffer. The amine-reactive group of SIAXX links to the calmodulin's lysine group. Then, the sample cell was assembled, and the HEPES buffer was used, with or without $CaCl_2$ (0.1 mM) and C28W peptide (50−100 nM).

2. Experimental Setup. Single-molecule fluorescence FRET and polarization measurements were performed on an inverted confocal microscope (Zeiss Axiovert 200) under ambient conditions.[43] Figure 2 shows the experimental setup schematics. A continuous-wave argon ion laser delivered the excitation light at 488 nm via a single-mode optical fiber. The beam was collimated after the fiber and passed through a quarter waveplate. The beam (circular polarized) was sent into the microscope, reflected up by a dichroic beam splitter (Chroma 505DCLP), and focused by a 100× oil immersion objective lens (Zeiss Fluar NA 1.3) onto the upper surface of a microscope coverslip (Bioptechs Inc., 0.17 mm thick). An $x-y$ closed-loop piezo position scanning stage was used to raster-scan the sample or to move a particular position of the sample over the laser focus. The fluorescence was collected by the same objective lens, passed through a long-pass filter (Chroma HQ515), and split into two components. This splitting was by one of two methods: (a) for the single-molecule FRET measurements, split by another dichroic beam splitter (Chroma 565DCLP), directed to two silicon avalanche photodiodes (APD; Perkin-Elmer, SPCM-AQR-16) with a 50-nm band-pass filter (Chroma HQ525/50m) at 525 nm for the donor channel and a 60-nm band-pass filter center at 630 nm for the acceptor channel, or (b) for the single-molecule fluorescence polarization measurements by a polarization beam-splitter cube (CVI Laser) directed to two APDs without filters. By using the photon stamping technique, the arrival time of each photon (Figure 3, insert) at the two APD was analyzed to obtain and identify the intensity trajectories (Figure 3A and 3B) of both channels, with the desired time resolution depending on the binning time.

3. Analysis of Single-Molecule FRET Efficiency Distribution. The laser beam was focused onto the sample solutions at least 10 μm above the glass surface into the solution. As the single molecules traversed the diffraction-limited laser focal region, fluorescence was obtained in the donor and acceptor channels separately in 500-μs bins (Figure 3A and 3B). Since a much higher concentration of C28W (~10 nM) was used, the average signal from the control experiment on the C28W-

(43) Hu, D.; Lu, H. P. *J. Phys. Chem. B* **2003**, *107* (2), 618−626.

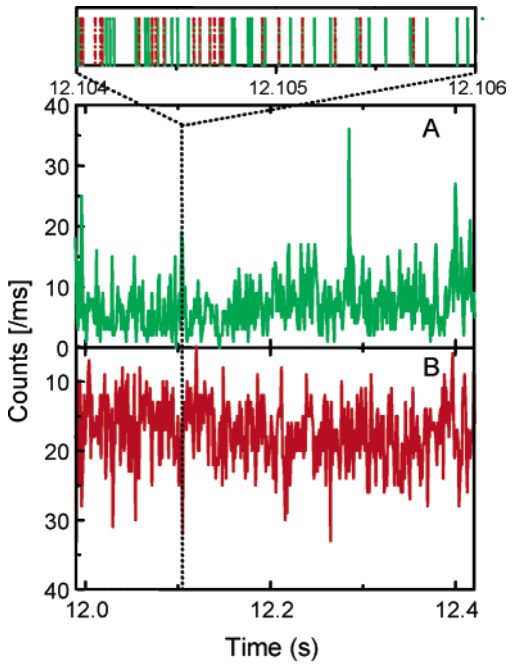

Figure 3. Single-molecule fluorescence correlation spectroscopy of protein−protein interactions: FlAsH labeled CaM interacting with Texas Red labeled C28W peptide. Examples of burst time trajectory collected in 1-ms bins, showing counts in donor (A) and acceptor (B) channels. *Insert* (top plot), arrival time of each photon (donor channel, green solid bar; acceptor channel, red dashed bar) within a bin time.

only sample was used as the background subtraction for the CaM/C28W sample. The signals $S_i(t)$ were corrected for background emission and donor/acceptor cross-talk due to overlapping emission:

$$S_i(t) = I_i(t) + B_i + \alpha_i I_j \tag{1}$$

where i, j is donor or acceptor, $B_{i,j}$ is the background, and $\alpha_{i,j}$ is the cross-talk efficiency between the donor and acceptor detection channels. Thus, the corrected donor/acceptor counts $I_i(t)$ were calculated by

$$I_i(t) = \frac{S_i(t) - \alpha_i S_j(t) - B_i + \alpha_i B_j}{1 - \alpha_i \alpha_j} \tag{2}$$

Then, the time trajectory of FRET, $E_{FRET}(t)$, can be calculated from $I_A(t)$ and $I_D(t)$, as shown in eq 3, where ϕ_A and ϕ_D are the emission quantum yields of acceptor and donor dyes, respectively, and η_A and η_D are the acceptor and donor detection efficiencies, respectively. Here, the correction factor for emission and detection efficiencies $(\phi_A \times \eta_A)/(\phi_D \times \eta_D)$ is ~1 under our experimental conditions. Single-molecule $E_{FRET}(t)$ is associated with the donor−acceptor distance $R(t)$ as in the case of eq 4:

$$E_{FRET}(t) = \frac{I_A(t)}{I_A(t) + I_D(t) \times \dfrac{\phi_A \times \eta_A}{\phi_D \times \eta_D}} \tag{3}$$

$$E_{FRET}(t) = \frac{{R_0}^6}{{R_0}^6 + R(t)^6} \tag{4}$$

where R_0 is the Förster radius, the donor−acceptor distance at which energy transfer is 50% efficient. For FlAsH and Texas Red pairs, an R_0 of ~48 Å was calculated from the spectral overlap of the donor fluorescence and acceptor absorption, assuming totally random relative orientation between the dipoles of both dye molecules. Although the Förster radius R_0 is calculated based on a few assumptions, the relative distance R/R_0 calculated from FRET efficiency is not affected by the assumptions.[44]

4. Single-Molecule FlAsH−CaM Fluorescence Polarization. With a polarization beam-splitter,[33] the two-channel intensity trajectories, at vertical or parallel polarizations related to the excitation polarization, $I_1(t)$ and $I_2(t)$, can be used to calculate the fluorescence polarization trajectories $P(t)$ for each single CaM protein tethered onto the hydrocarbon-modified glass surface:

$$P(t) = \frac{I_1(t) - fI_2(t)}{I_1(t) + fI_2(t)} \tag{5}$$

where f is a weighing factor used to balance the two channels and determined by recording the emission from isotropic bulk samples. Then, the autocorrelation function can be calculated and normalized for each fluorescence polarization trajectory by eq 6:

$$\begin{aligned} C(t) &= \langle \Delta P(0) \Delta P(t) \rangle / \langle \Delta P(0)^2 \rangle \\ &= \langle (P(0) - \langle P \rangle)(P(t) - \langle P \rangle) \rangle / \langle (P(0) - \langle P \rangle)^2 \rangle \end{aligned} \tag{6}$$

Results and Discussion

Calcium-activated CaM is capable of binding to a target peptide, such as C28W. It has been suggested that the initial recognition and association of the CaM and target peptide reside in the carboxyl-terminal (C-terminal) domain of CaM; the N-terminal binding domain of CaM then binds to the peptide to form a CaM/C28W complex.[19,39] The C-terminal domain of CaM has previously been proven to have a higher affinity to target protein/peptides (about 100 times higher), including C28W, than the N-terminal domain.[22] Upon association of C28W with the binding cleft in the C-terminal domain of CaM, the N-terminal domain may bind around the target peptide.[22,45,46] Ensemble-averaged measurements have provided some evidence of the existence of a flexible conformational fluctuation of the N-domain binding to peptide targets. For example, based on the frequency-domain anisotropy measurements of bound FlAsH dye in the N-terminal of CaM proteins, the rotational times of CaM, Ca-CaM, and CaM/C28W have been reported as 10, 15, and 17 ns, respectively.[19] However, there is no real-time observation and identification on the intermediate state of CaM targeting processes. There is a high possibility that the N-terminal may involve binding and unbinding motions when the C-terminal remains associated with the peptide target, as in the case of the B and C states shown in Figure 1.

FRET measurements are able to probe the distance changes and fluctuations between donor and acceptor dyes, normally in a range from ~2 nm to ~10 nm, because the variation in distance results in changes in the efficiency of the energy transfer from the donor to the acceptor. For FlAsH labeled CaM and Texas Red labeled C28W pairs, the possibility of FRET from FlAsH to Texas Red is negligible when there is no direct interaction between CaM and C28W. This is because normally they pass by each other at the diffusion time scale, and the

(44) A threshold criterion was applied to the photon counts of both channels before a calculation of FRET efficiency, to remove experimental points where the photon counts are due to the fluctuation of background and/or cross-talk from the other channel. The threshold criterion equals 2× the standard deviation from the background and the cross-talk, assuming that the uncertainty is due to photon-counting shot noise in the background and the cross-talk.

(45) Crivici, A.; Ikura, M. *Annual Review of Biophysics and Biomolecular Structure* **1995**, *24* (1), 85−116.
(46) Ehrhardt, M. R.; Urbauer, J. L.; Wand, A. J. *Biochemistry* **1995**, *34*, 4 (9), 2731−2738.

average distances between FlAsH and Texas Red are far beyond the largest FRET-resolvable distance (>10 nm). Only when CaM and C28W interact or bind to each other can the distance between FlAsH and Texas Red fall in the FRET-resolvable range (2 to 10 nm). Since the FlAsH dye is labeled close to the end of the N-terminal domain of the CaM protein and the Texas Red dye is labeled to the N-terminal end of C28W (Figure 1), any change in interaction states between CaM and C28W, i.e., intermediate states or final states, and any change in CaM conformation (as shown in Figure 1) will result in a difference in FRET efficiency between the labeled FlAsH and Texas Red dyes. Therefore, the single-molecule FRET experiments of FlAsH labeled CaM and/or Texas Red labeled C28W are expected to provide insights into the distributions of distances between the FlAsH and Texas Red dye molecules and, thus, the distance between the N-terminal domains of CaM and bound C28W. This information is expected to reveal the conformation change of CaM and the substates or intermediate states of interaction between the CaM and C28W.

To probe the complexes of FlAsH labeled CaM and Texas Red labeled C28W, we chose a concentration for CaM/C28W of about 0.2 nM for the single-molecule binding assay. Under such experimental conditions, unbound CaM and C28W could also contribute to the FRET efficiency distribution calculated from the fluorescence pulses in the donor and acceptor channels.[47] Therefore, control experiments on samples composed of FlAsH labeled CaM only and Texas Red labeled C28W only were performed under the same conditions as those for mixed samples. Most of the bursts from FlAsH labeled CaM alone give an FRET efficiency near 0, with only a negligible number of bursts with an FRET efficiency between 0.1 and 0.9. Similarly, while most of the bursts from Texas Red labeled C28W alone give an FRET efficiency near 1, there are only a negligible number of bursts that give an FRET efficiency between 0.1 and 0.9. Therefore, the contribution of FRET efficiency in the range 0.1−0.9 from unbound CaM and C28W is minimal. Figure 4A and 4B show the distributions of FRET efficiency and the calculated relative distance R/R_0 distribution for the dye-labeled CaM/C28W complex. Both distributions are asymmetric and elongated to one side. It is evident that the distribution contains more than one component, although we have only analyzed the distribution by fitting to two Gaussian peaks. Although both the distance difference and orientation factor difference contribute to the FRET efficiency difference, we attribute that the distance difference plays the major role.[48] The relative distance distribution (Figure 4B) was obtained by a fit of two Gaussian peaks with significantly different mean

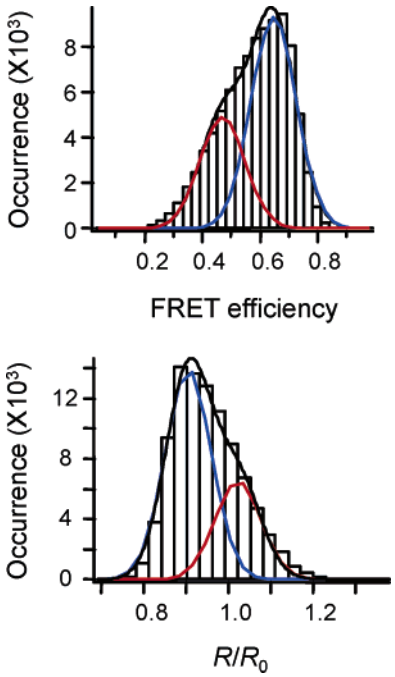

Figure 4. Distributions of single-molecule FRET efficiency (A) and calculated relative donor−acceptor distance (R/R_0) (B). The blue and red curves are the Gaussian components used to fit the distributions, and the black curve is fitted results.

distances associated with the different R/R_0 ratio. The distance changes in a wide range from 40 to 53 Å. We attribute the major peak corresponding to a shorter distance between the two dyes to the tightly binding state of the CaM/C28W complex, where CaM adopts the compact conformation of both N- and C-terminal domains binding to C28W. The minor peak indicates that some intermediate states exist with a larger distance between the two N-terminal domains of CaM and C28W so that the interaction between cannot be as strong as that in the compact conformation of CaM. We note that although the qualitative assignment of the two distance distributions associated with the comformational states is observable (Figure 4B), a quantitative assignment of an exact distance range can be associated with significant error bars because of the relatively weak signals, spectral fluctuation, and photobleaching.[4]

To further characterize the intermediate interaction state between CaM and C28W and to study the dynamics of the interactions, single-molecule fluorescence polarization measurements were carried out on FlAsH labeled CaM tethered on the surface of glass coverslips. Fluorescence polarization indicates the orientation of single emitting dye molecules,[49−51] so the rigid tetracoordinate linkage of FlAsH to CaM (Figure 1 inset) ensures that the measured fluorescence polarization trajectories can yield information about the rotational and conformational dynamics of the CaM host protein, particularly the N-terminal domain of CaM where FlAsH embeds. It has been demonstrated at the ensemble-averaged level that FlAsH labeled CaM in buffer solution showed a fluorescence anisotropy change upon binding to C28W, which implicates a rotation-rate change of CaM in

(47) From the equilibrium: CaM + C28W ↔ CaM/C28W, and the equilibrium constant $\sim 1 \times 10^8$ M^{-1}, the final concentration of each component in the mixture of CaM and C28W in the single-molecule FRET experiments are expected to be approximately C28W 9.802 nM, CaM 0.202 nM, and CaM/C28W 0.198 nM, respectively. Though, the expected concentration ratio between CaM and CaM/C28W is close to 1:1, in the FRET experiments, the CaM/C28W appeared at a lower concentration, due to reasons, such as (1) the C28W peptide is not 100% labeled and (2) the interaction between CaM and C28W is in dynamics, and there are some times that CaM/C28W becomes dissociated.

(48) First, the energy transfer acceptor Texas Red is linked to the peptide by a single bond and should be very flexible. Both molecular structure modeling and time-resolved anisotropy of the tethered Texas Red have shown a large rotational freedom of the Texas Red probe (see Supporting Information for detail). Its orientation should be averaged within the time bin and is unlikely to contribute to a large change of the FRET efficiency, reflected by 2.3 times in the energy transfer rate (FRET efficiency change from 0.45 to 0.65). Second, the energy transfer donor FlAsH is locked in the matrix of the N-terminal domain of CaM, and its orientation change has to be induced by the conformational change of CaM.

(49) Bartko, A. P.; Xu, K.; Dickson, R. M. *Phys. Rev. Lett.* **2002**, *89* (2), 026101−026104.
(50) Adachi, K.; Yasuda, R.; Noji, H.; Itoh, H.; Harada, Y.; Yoshida, M.; Kinosita, K. J. *Proc. Natl. Acad. Sci. U.S.A.* **2000**, *97* (13), 7243−7247.
(51) Yasuda, R.; Noji, H.; Kazuhiko Kinosita, J.; Yoshida, M. *Cell* **1998**, *93* (7), 1117−1124.

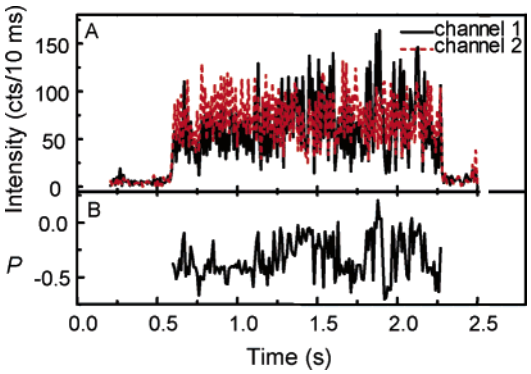

Figure 5. Single-molecule fluorescence polarization measurements of the protein−protein interactions: FlAsH labeled CaM interacting with non-labeled C28W peptide. (A) Fluorescence intensity trajectories, calculated from the arrival time of photons with a time-bin resolution of 10 ms: channel 1, black solid line; channel 2, red dashed line. (B) Fluorescence polarization trajectory, calculated from the intensity trajectories of (A) using eq 1.

solution.[19,39] Here, we used single-molecule polarization spectroscopy to probe the rotational and conformational dynamics of CaM interacting with C28W. In the single-molecule experiments, CaM was covalently tethered to a hydrocarbon-modified glass surface, as discussed above.[33] The advantages of the experiments using the FlAsH labeled CaM tethered on the surface of glass are that the linker still gives the linked CaM the freedom of rotation and the photon-stamping time trajectories from individual molecules are recorded in order to reveal the polarization fluctuation dynamics. Furthermore, the interaction with C28W can induce fluctuations in the rotational restriction and cause the changes in the fluorescence polarization discussed below. Figure 5A and 5B show typical two-channel fluorescence intensity trajectories and the corresponding polarization trajectory of a single FlAsH labeled CaM protein in a HEPES buffer solution containing $CaCl_2$ (0.1 mM) and the C28W peptide (70 nM). Here, the fluctuation in fluorescence intensity and polarization on a millisecond time scale was observed, which we attributed to conformational motions of the N-terminal domain of the CaM protein during the measurement. In control experiments, both apo-CaM and Ca^{2+}-CaM were also studied, using only a HEPES buffer and a HEPES buffer/$CaCl_2$ (0.1 mM), respectively. Their polarization trajectories were also analyzed in comparison with the polarization trajectories of CaM interacting with C28W.

Several factors must be taken into consideration. First, the covalent bifunctional linker to tethered CaM on the modified glass surface still gave the linked protein the capability of rotational motion,[43] which agrees with previous experiments that obtained the single-molecule fluorescence anisotropy measurements.[33] Second, the polarization experiments in this work provide different information from our previous nanosecond anisotropy work. Since the rotational correlation time of CaM, either saturated with calcium ions or not, is on the order of nanoseconds,[19,21,24,52] the polarization calculated in this work (Figure 5B) actually reports an averaged orientation of the individual molecules over each time bin of the trajectory, usually in the millisecond time scale. If the molecule reached all orientations nonrestrictively within the time bin, the polarization was zero. If the molecule's rotation had a spatial restriction, the polarization had a possible value between −1 and 1. On the other hand, the nanosecond rotation rate had no direct contribution to the value of polarization. Finally, the fluorescence intensity trajectories inevitably contain photon shot noise. Therefore, the polarization trajectory calculated from the intensity trajectory also had an error due to photon shot noise, which gave additional fluctuation to the polarization trajectory and broadened the distribution of polarization.

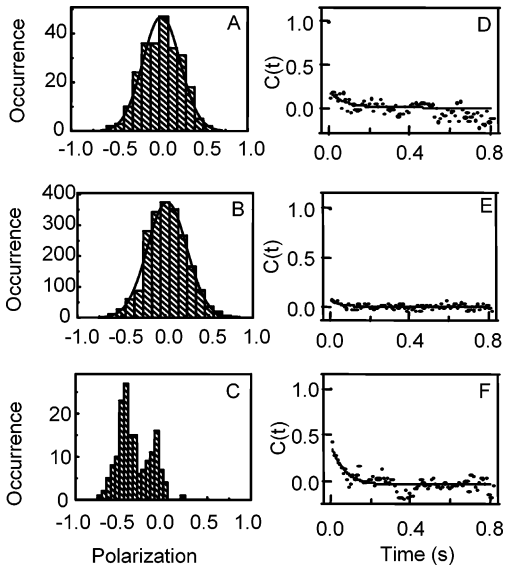

Figure 6. Typical fluorescence polarization distributions and autocorrelation functions of single FlAsH labeled CaM: (A) apo-CaM, (B) Ca^{2+}-CaM, (C) CaM/C28W. Corresponding autocorrelation functions were calculated from polarization trajectories: (D) apo-CaM, (E) Ca^{2+}-CaM, (F) CaM/C28W.

To identify and analyze the protein conformational dynamics, we obtained a fluorescence polarization distribution of each single CaM protein and calculated the autocorrelation function $C(t)$ for each single-molecule polarization trajectory of $P(t)$. Figure 6 shows a typical single-molecule fluorescence polarization distribution and the autocorrelation functions of the polarization trajectories of single CaM protein molecules under three assay conditions: Ca^{2+} free CaM (apo-CaM), Ca^{2+}-activated CaM (Ca^{2+}-CaM), and complexes (CaM/C28W) of Ca^{2+}-activated CaM and C28W peptides. The histograms of the fluorescence polarizations of both apo-CaM (Figure 6A) and Ca^{2+}-CaM (Figure 6B) have a similar broad Gaussian-type distribution with a mean at $P = 0$, which indicates that the CaM tethered to the modified glass surface at both conditions was fully flexible in motion. In contrast, the histogram of polarizations of CaM/C28W (Figure 6C) has an asymmetric distribution below $P = 0$, with two distinguishable peaks, which strongly suggests that the CaM diffusional and rotational motions had been polarized or restricted under CaM/C28W interactions.

It is important that the contribution from shot noise has to be determined before the interpretation of the rotation motions of the single molecules. One method to evaluate the shot noise contribution is to propagate the fluctuation of the intensity counts of I_1 and I_2 through eq 5. However, the noise propagation through eq 5 is hard to evaluate accurately because of the fluctuation of I_1 and I_2. By an approximation, we estimated that photon shot noise was the major factor of the broadening of peaks in Figure 6A and 6B, but not in Figure 6C, as the autocorrelation amplitudes indicated (Figure 6D−6F), which suggests that the fluctuation of the polarization of the molecule

(52) Sun, H.; Yin, D.; Squier, T. C. *Biochemistry* **1999**, *38* (38), 12266−12279.

in Figure 6C was beyond noise and might have been due to the fluctuation in rotational motion. As discussed above, polarization is the indictor of spatially restricted rotation. Therefore, the fluctuation of polarization suggests the fluctuation of the rotational restriction. Since the CaM/C28W complex should have nanosecond rotation correlation time in solution, the rotational restriction is most likely due to the interaction of the complex with the surface. The second method is to evaluate the noise of P from the autocorrelation function of P. Because shot noise is uncorrelated from point to point in the time sequence, shot noise shows amplitude in only the first point of the autocorrelation. If the change of P was purely from the shot noise of I_1 and I_2, the autocorrelation function would drop to zero after the first data point at time zero. In Figure 6D and 6E, the autocorrelation function's amplitude from the second point is small (0.2 and 0.1). The change of P was mostly due to the shot noise of the fluorescence intensity. The data suggest that, in agreement with previous work,[33] the surface tethering of CaM by a covalent bonding does not affect the free rotation of the N-terminal domain of CaM without spatial restriction in the case of the apo-CaM and Ca^{2+}-CaM.[33,43] In contrast, the autocorrelation function of single CaM/C28W complexes has a significantly larger amplitude (0.45).

We were able to fit the autocorrelation function (solid curves in Figure 6D−6F) to obtain polarization fluctuation kinetic rates, assuming single-exponential decays. The autocorrelation functions in Figure 6F clearly show millisecond time-scale decay kinetics, indicating that there were exchanges between the rotational states or restrictions of CaM/C28W in the millisecond time scale. In other words, the binding state of CaM and C28W was likely involved in the N-terminal domain's fluctuating between a bound and a loosely or partially bound state while the overall complex was still associated, causing the fluctuation in the restriction of rotation (Figure 1). Furthermore, the distribution of P is not a Gaussian centered at zero (Figure 6C), and the autocorrelation of P has a larger amplitude of $C(t)$ decay at $t > 0$, indicating that there are more rotational restrictions observable in the millisecond time scale for CaM/C28W than that for apo-CaM and Ca^{2+}-CaM. Such a difference is most likely caused by protein−peptide interactions between CaM and C28W.[53] The fact that the autocorrelation amplitudes of apo-CaM and Ca^{2+}-CaM are much smaller than that of CaM/C28W suggests that the possible fluctuation in rotation states or restrictions is not significant. The correlated results of single-molecule polarization histograms and autocorrelations (Figure 6) suggest that the apo-CaM and Ca^{2+}-CaM both rotate freely in buffer solution at the observation time scale of milliseconds.

To further identify and characterize the motions of the N-terminal domain binding and unbinding of the target peptide, we collected the fluorescence intensity and polarization trajectories of more than 50 single molecules for CaM proteins in each of the three assay conditions described above. Autocorrelation functions calculated from the fluorescence polarization trajectories of these molecules, excluding the first point $C(0)$ at $t = 0$, were fitted to a single-exponential decay, $C(t) = A_\tau \exp(-kt)$. Figure 7 shows the distributions of A_τ for apo-CaM, Ca^{2+}-actived CaM, and CaM/C28W, as well as for those of the decay rates (k). The A_τ shows the fluctuation amplitude, excluding shot noise and contributions from fast fluctuations beyond the experimental measurement time resolution. The distributions of A_τ for both apo-CaM (Figure 7A) and Ca^{2+}-CaM (Figure 7B) are similar, mostly between 0 and 0.2, while the latter is slightly wider. In contrast, the A_τ values for CaM/C28W (Figure 7C) distribute much more broadly, from 0 to 0.6. The corresponding distributions (Figure 7D−7F) of kinetic rates derived from the fluorescence polarization autocorrelation functions similarly cover the whole measurable time window from milliseconds to seconds, which is limited by the fluorescence trajectory lengths and photon emission rates. To further illustrate the results of autocorrelation fitting, a two-dimensional histogram of autocorrelation amplitude A_τ versus autocorrelation rates (k) is plotted for the three assay conditions (Figure 8). The 2D distributions for apo-CaM (Figure 8A) and Ca^{2+}-CaM (Figure 8B) show similar distributions. In contrast, the distribution (Figure 8C) for single-molecule CaM/C28W complexes clearly shows a protuberant component beyond the major part of the distribution similar to that for apo-CaM (Figure 8A) and Ca^{2+}-CaM (Figure 8B). This component has a larger amplitude and falls in a rate range of $10-100\ s^{-1}$, possibly indicating slow fluctuations in the binding states between the CaM protein and the C28W peptide. For those molecules with smaller A_τ, their autocorrelation rates should have larger errors in fitting. However, a large A_τ indicates a more reliable fitting of the kinetics. Since the hydrodynamic shape and protein surface structure of the tightly bound state of CaM/C28W (Figure 1C) is similar to those of apo-CaM and Ca^{2+}-CaM, the possible surface restriction on the rotation motions is most likely on the C-terminal bound state of CaM/C28W (Figure 1B). Dynamics at the sub-millisecond and millisecond time-scale were also reported for apo-CaM, Ca^{2+}-CaM, and the CaM-peptide using single-molecule spectroscopy.[32,34] The dynamics in fluorescence polarization revealed by autocorrelation functions imply the presence of considerable heterogeneity in the rotation of the CaM peptide. The rate of the polarization fluctuation might be

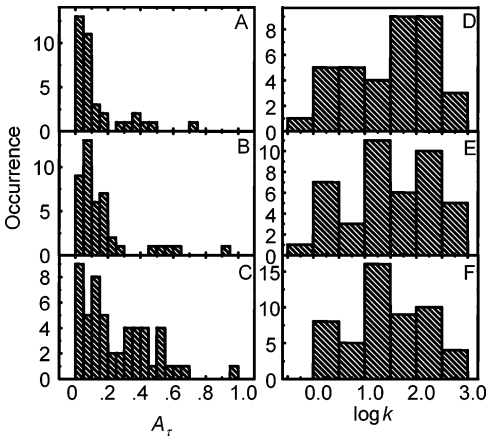

Figure 7. Distributions of amplitudes A_τ and decay rates k (s^{-1}) of autocorrelation functions of the single-molecule fluorescence polarization trajectory of (A) apo-CaM, (B) Ca^{2+}-CaM, and (C) CaM/C28W; distributions of the corresponding decay rates of the autocorrelation functions for (D) apo-CaM, (E) Ca^{2+}-CaM, and (F) CaM/C28W.

(53) Since the lysines at the central helix elements of CaM are more accessible to the bifunctional linker molecules used in the tethering process, most CaM molecules in the polarization measurements are expected to be linked to the glass surface through its central part. Therefore, once the C28W peptide interacts with CaM, especially in the intermediate state (if exist), the N-terminal domain of CaM changing from unbound to bound with C28W, the restriction on the conformation freedom of the N-terminal domain of CaM changes dramatically. This can be reflected by the distribution and dynamics of fluorescence polarization of the FlAsH dye molecules labeled there.

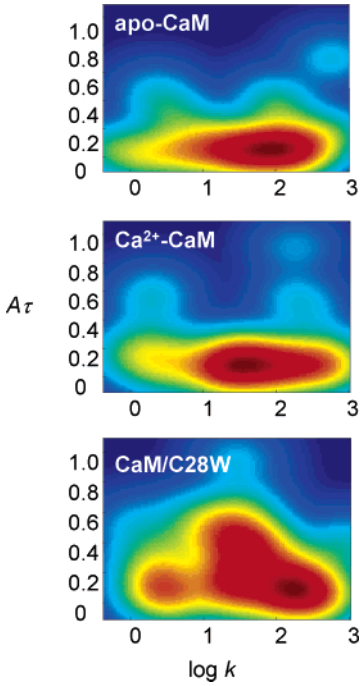

Figure 8. Two-dimensional distributions of correlated decay rates (k, s^{-1}) and amplitudes (A_τ) of autocorrelation functions of fluorescence polarization trajectories for (A) apo-CaM, (B) Ca^{2+}-CaM, and (C) CaM/C28W.

affected by other factors, such as conformational changes of the complex and surface interaction. Although this rate has not been unambiguously interpreted, the difference between CaM/C28W (Figure 8C) and CaM alone (Figure 8A and B) is clear, which is induced by C28W. The binding of CaM with many target proteins and peptides, including C28W, results in conformation fluctuations (as shown in Figure 1B and 1C)[11,15,22,45,46,54,55] and consequently affects interaction of the complex with the glass surface. It is reasonable that significant conformational changes likely require higher activation energy involving slower kinetic rates than that of the nanosecond fast subtle change and rotational dynamics.[19,21,24,52] Our observation of the bound and loosely bound states of the N-terminal domain of CaM to the target peptide is in agreement with present high-resolution structures of apo-CaM and Ca^{2+}-CaM that demonstrate heterogeneity with respect to interhelical angles within each globular domain of CaM[56−59] and changes in average global structure upon the activation of CaM by a calcium ion.[8−10,18,60] Further study of specifically monitoring the polarization of C28W will provide more information about the binding states of CaM/C28W.

Using a rotationally locked dye probe, FlAsH anchored in the N-terminal matrix of CaM, to probe the domain conformational motions in a single-molecule fluorescence anisotropy measurement is novel and promising. However, we must note that the sensitivity and selectivity of using this approach to resolve the conformational change dynamics are still preliminary. For example, the most precise way to apply this approach is to conduct a single-molecule nanosecond or sub-nanosecond time-resolved anisotropy measurement of a freely diffusing CaM/C28W complex in solution, and the same individual complex molecule has to be followed in solution during the measurement; this is still technically not possible at present. What we have demonstrated in this paper is to tether the single-molecule CaM to a surface and measure the static polarization changes of the CaM under single-molecule CaM/C28W binding assay conditions. Obviously, additional technical development will be needed to achieve a protein conformational dynamics measurement by single-molecule anisotropy. Presumably, new technical developments aiming to achieve automatic three-dimensional tracking and single-photon stamping of specific individual molecules will help on meeting this technical challenge in the future.

Conclusion

Using the unique dye label, FlAsH, which permits selective and rigid binding to the N-terminal domain of CaM, and applying single-molecule FRET and fluorescence polarization measurements, we studied the interactions between CaM proteins and C28W peptides and compared the conformational dynamics of CaM proteins in three assay systems: apo-CaM, Ca^{2+}-CaM, and CaM/C28W. In particular, the conformational fluctuations and interactions involving the N-terminal domain of CaM, where the FlAsH dye was labeled, were investigated in detail. The single-molecule FRET study revealed that there were intermediate states in the interaction between CaM and C28W. The broad distribution of the distance between the N-terminal domains of CaM and C28W of the complexes, measured by FRET efficiency for the intermediate states, indicated conformational fluctuations between two distinguishable conformational states. In single-molecule fluorescence polarization experiments, although only CaM/28W showed a clear deviation from a single-Gaussian distribution, dynamics of CaM at a millisecond time scale in all three situations were revealed by polarization autocorrelation functions. The observed difference in the polarization distribution of CaM/C28W from that of apo-CaM and Ca^{2+}-CaM is further evidence of conformational fluctuations between bound and loosely bound states in the CaM/C28W complexes, while the C-terminal domain of CaM is overall still associated with the C28W peptide. Such fluctuations were found to be as slow as tens of milliseconds to hundreds of milliseconds, which is a time range that can be detected by single-molecule fluorescence trajectories and an autocorrelation function calculation. The results suggest a high inhomogeneity in protein conformational dynamics and fluctuations in protein−peptide (protein) interactions in the cell-signaling systems. These dynamic behaviors of the protein−protein interactions cannot be observed by ensemble-averaged measurements but only by single-molecule approaches.[33,61,62] It is likely that the fluctuating protein−protein interactions involving bound and loosely bound states are general and essential for a cell-signaling process, as we have observed with

(54) Seaton, B. A.; Head, J. F.; Engelman, D. M.; Richards, F. M. *Biochemistry* **1985**, *24*, 6740−6743.
(55) Heidorn, D. B.; Seeger, P. A.; Rokop, S. E.; Blumenthal, D. K.; Means, A. R.; Crespi, H.; Trewhella, J. *Biochemistry* **1989**, *28*, 6757−6764.
(56) Chou, J. J.; Li, S.; Klee, C. B.; Bax, A. *Nature Structural Biology* **2001**, *8* (11), 990−997.
(57) Wilson, M. A.; Brunger, A. T. *J. Mol. Biol.* **2000**, *301*, 1237−1256.
(58) Jaren, O. R.; Kranz, J. K.; Sorensen, B. R.; Wand, A. J.; Shea, M. A. *Biochemistry* **2002**, *41* (48), 14158−14166.
(59) Fallon, J. L.; Quiocho, F. A. *Structure* **2003**, *11* (10), 1303−1307.
(60) Finn, B. E.; Evenäs, J.; Drakenberg, T.; Waltho, J. P.; Thulin, E.; Forsén, S. *Nature Structural Biology* **1995**, *2* (9), 777−783.
(61) Tan, X.; Nalbant, P.; Toutchkine, A.; Hu, D.; Vorpagel, E. R.; Hahn, K. M.; Lu, H. P. *J. Phys. Chem. B* **2004**, *108* (2), 737−744.
(62) Lu, H. P.; Iakoucheva, L. M.; Ackerman, E. J. *J. Am. Chem. Soc.* **2001**, *123* (37), 9184−9185.

similar fluctuating biomolecular interactions in cell signaling for other systems.[61,62] Although more evidence from both dynamic and static analyses has been reported,[8,11−31,33,61,62] a definitive answer has yet to come. Presumably, a fluctuating binding rather than a static and tight binding would be more energetically efficient and kinetically effective for a consecutive protein−protein interaction cascade pathway in living cells.

Acknowledgment. We thank Thomas Squier and Baowei Chen for helpful discussions and for providing us with the C28W peptide and FlAsH labeled CaM. This work was supported by the Chemical Science Division of the Office of Basic Energy Sciences, U.S. Department of Energy (DOE), and was supported by the Laboratory Directed Research and Development Program of the Pacific Northwest National Laboratory, operated for the U.S. Department of Energy by Battelle Memorial Institute under Contract DE-AC06-76RLO1830.

Supporting Information Available: Figure showing open and closed structure of CaM−C28W with Texas Red label on the peptide, and figure showing time-resolved anisotropy decay of Texas Red in water and tethered Texas Red in calmodulin/C28W in buffer solution. This material is available free of charge via the Internet at http://pubs.acs.org.

JA057005M